



Upper Mantle Discontinuities Underneath Central and Southern Mexico

Xyoli Pérez-Campos^{1,2}, Robert W. Clayton²

¹ Departamento de Sismología, Instituto de Geofísica, Universidad Nacional Autónoma de México, Ciudad Universitaria, Coyoacán; Mexico, D. F. 04510, MEXICO, xyoli@geofisica.unam.mx

² Seismological Laboratory, California Institute of Technology, Pasadena, CA 91125, USA



INTRODUCTION

Central and southern Mexico is tectonically characterized by the subduction of the Cocos plate under North American plate with an average rate of ~6 cm/yr. The subduction angle varies along the trench, from a high angle at the north, to a horizontal subduction in central Mexico and back to a high angle to the south (Pardo & Suárez, 1995).

Cocos subduction started at the beginning of the Miocene, when the Farallon plate evolved into the Cocos plate. The subduction of the East Pacific Rise produced a slab window and a slab tear that propagated laterally eastward. This is evident from the volcanism migration observed in the Trans Mexican Volcanic Belt (TMVB) evolution. Currently, the slab is rolling back, as indicated by a southern migration of the TMVB volcanism and the lack of compressional stresses in the overriding plate.

The slab geometry has been delineated by seismicity (e.g., Pardo & Suárez, 1995), tomography (Gorbatov & Fukao, 2005; Husker & Davis, 2009) and receiver functions (Pérez-Campos et al., 2008; Kim et al., 2010; Melgar & Pérez-Campos, 2011). The most striking feature of the slab is its flatness under central Mexico, for 250 km from the trench (Pérez-Campos et al., 2008). After this, right before the TMVB, the slab subducts rapidly into the upper mantle with a steep angle of 70°, reaching a depth of ~410 km at a distance of 380 km from the trench. The slab seems to end at a depth of 500 km (Pérez-Campos et al., 2008; Husker & Davis, 2009).

The goal of this work is to determine the presence of the slab in the mantle transition zone (MTZ), between the seismic discontinuities at 410 km and 660 km, its interaction with the discontinuities and its roll on hydrating the upper mantle in the region.

DATA

We use teleseismic data from three major experiments that have taken place in central and southern Mexico: the Meso American Subduction Experiment (MASE), the Veracruz-Oaxaca (VEOX) experiment and the Mapping the Rivera Subduction zone (MARS) experiment; we also use data from broadband permanent stations in central and southern Mexico of the Servicio Sismológico Nacional (SSN, National Seismological Service in Mexico), and from two temporary stations installed for this purpose (we will refer them as CONA) (Fig. 1). MASE operated from 2005 to 2007, VEOX from 2007 to 2009, MARS from 2005 to 2006, some SSN data are available since 2001, finally CONA stations were on the field for three and one year. In total, we were able to obtain 6032 receiver functions (RFs).

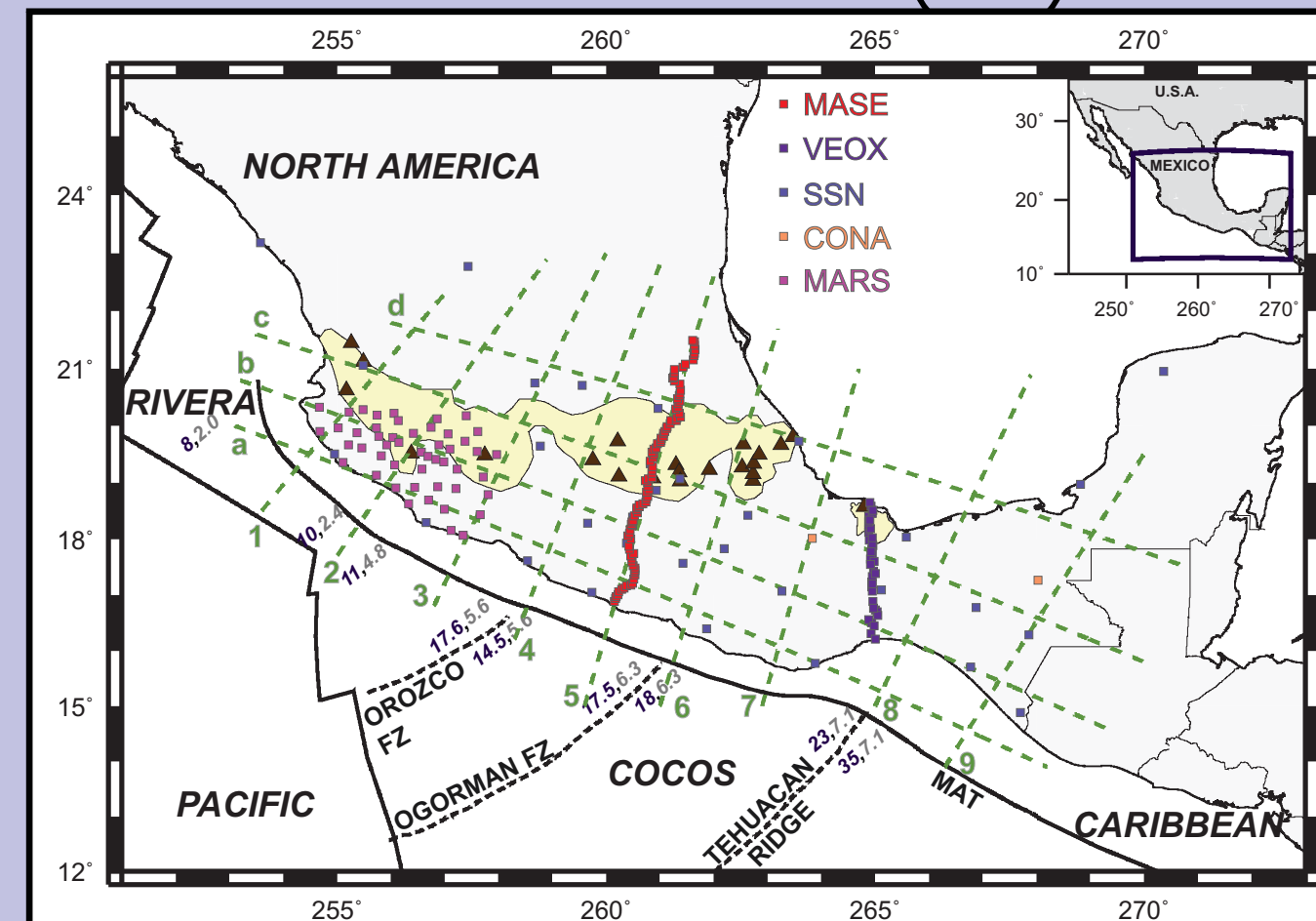


Figure 1. Station locations (squares). The yellow area denotes the location of the TMVB and the Tuxtias Volcanic Belt; brown triangles denote active volcanoes. Profiles 1 to 9 and a to d are shown in Fig 5. Numbers next to the trench give age in Ma (in purple) and subducting rate in cm/yr (in gray).

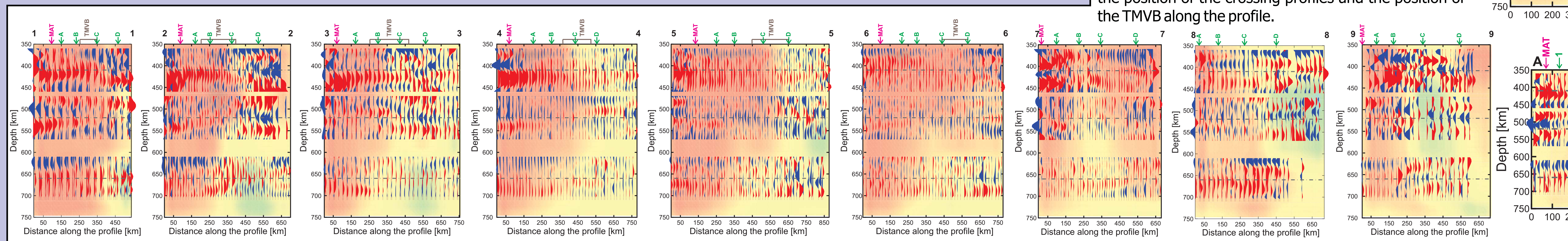
Topography of the Discontinuities

Figure 4 shows the topography of the upper mantle discontinuities and the thickness of the MTZ. The top of the MTZ is delimited by a seismic discontinuity at an average depth of 424±11km, this is 14 km deeper than the global average. Its topography shows one interesting feature uplift directly beneath central Mexico, where the slab reaches the 410 discontinuity according to the seismic tomography by Husker & Davis (2009). Two other regions of uplift are also observed, one at the northwest and the other one at the southeast. These correspond to presence of cold material according to seismic tomography by Gorbatov & Fukao (2005).

The 660 discontinuity shows an average depth of 656±17 km depth, which is close to the global average. However, it shows a depression over a large area under central Mexico, indicating the possibility of cold material sitting in the 660 discontinuity.

In general, the MTZ under central Mexico, south of the TMVB seems to be affected by the presence of cold material, making it slightly thicker (~15 km) than the global average (Fig. 4).

Figure 5 shows a series of profiles from west through east (from 1 through 9) and from south through north (from a through d). The 410, 520 and 660 global discontinuities are indicated. There is a striking correspondence between the RF nature and the tomography. RFs in the region of fast (cold) material show more complicated nature. Although intermittent, a low velocity layer (LVL) might be depicted above the 410 discontinuity, especially near where interaction seems to occur between cold material and the 410 discontinuity.



ABSTRACT

Central and southern Mexico are affected by the subduction of Cocos plate beneath North American plate. The MesoAmerican Subduction Experiment (MASE) and the Veracruz-Oaxaca (VEOX) project have mapped the geometry of the Cocos slab. It is characterized in central Mexico by a shallow horizontal geometry up to ~300 km from the trench, then it dives steeply (70°) into the mantle, to an apparent end at 500 km depth. In contrast, some 400 km to the south, the slab subducts smoothly, with a dip angle of ~26° to a depth of 150 km. We use receiver functions from teleseismic events, recorded at stations from MASE, VEOX, and the Servicio Sismológico Nacional (SSN, Mexican National Seismological Service) to map the upper mantle discontinuities and properties of the transition zone in central and southern Mexico. We also use data from the Mapping the Rivera Subduction Zone (MARS) Experiment to get a complete picture of the subduction regime in central Mexico and compare the mantle transition zone in a slab-tear regime.

Analysis of the Converted Phases

We employed the receiver function technique (Vinnik, 1977), with a data window that is 120-s length, starting 30 s before the P-wave onset. The three components (Z, N, E) are rotated to a P-polarization coordinate system (L, Q, T). We then performed the deconvolution of the Q component by the L component in the time domain (Ligorria & Ammon, 1999), using a Gaussian filter with parameter of 0.25. We chose the best RF based on the fit of the estimated Q component and the observed signal, keeping only those with 70% or higher resemblance. In order to enhance the mantle discontinuity arrivals, we further filtered the RF between 0.025 and 0.3 Hz (Fig. 2).

Following Dueker & Sheehan (1997), we stacked the RF according to their common conversion points (CCP). We used iasp91 (Kennett & Engdahl, 1991) as the reference velocity model to backproject the RFs and identify their conversion points at the 410 and the 660 discontinuities (Fig. 3). Based on Gilbert et al. (2003), we generated a 0.5° x 0.5° grid and stacked, for each discontinuity, the RFs within a distance of 1.5°, which means 66% overlap. The number of RFs at each node is shown in Fig. 3, the minimum number allowed is 10; as expected, the regions around the seismic experiments have better coverage. We obtained the mean RFs and its confidence interval by bootstrapping the RFs at each node (Efron & Tishirani, 1993).

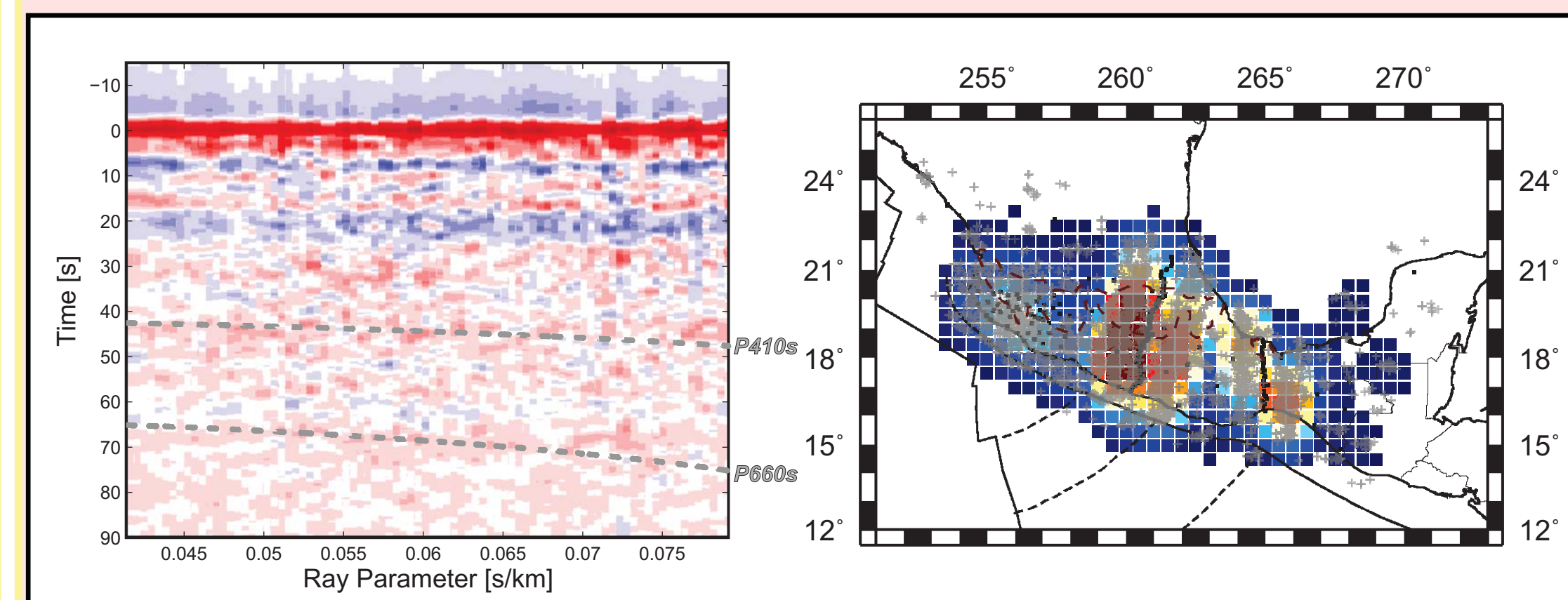
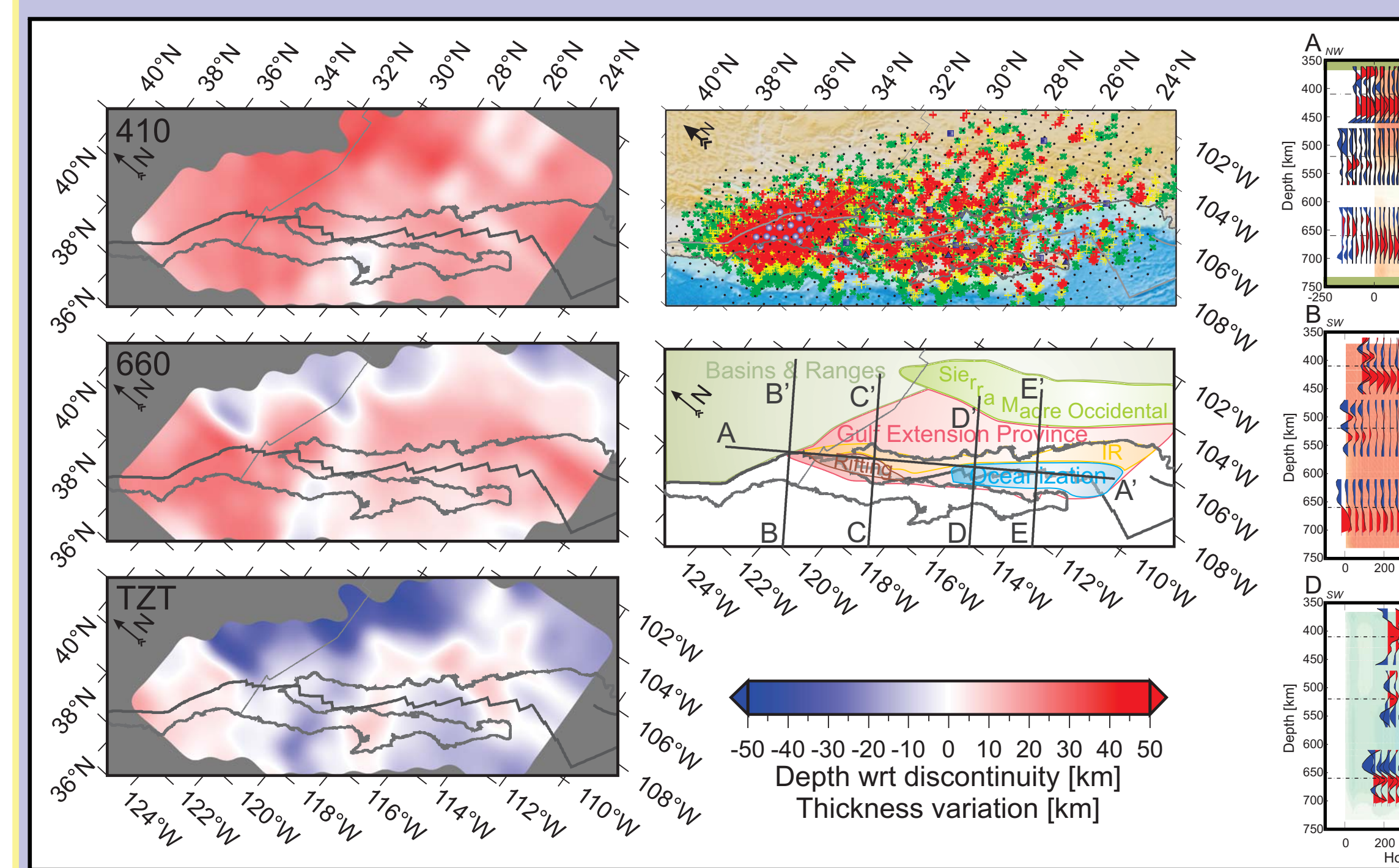


Figure 2. Receiver functions stacked by ray parameter. The RFs have been filtered between 0.025 and 0.3 Hz. The theoretical arrivals for the 410 (P410s) and the 660 (P660s) discontinuities are denoted by gray dashed lines.

Figure 3. Number of RFs per node for the 410 (top) and the 660 (bottom) discontinuities. The minimum allowed for the stacking was 10. The gray crosses denote the piercing points of the RFs at the depth of the discontinuity.



Discussion and Conclusions

Cocos slab seems to interact with the MTZ in an intermittent fashion rather than spatially continuous. In central Mexico, the slab penetrates the 410 discontinuity in the predicted spot by the recent seismic tomography of Husker & Davis (2009). Although this tomography shows a truncated slab at 500 km, a global tomography by Li et al. (2008) shows a persistent fast anomaly in the region that interacts with the 660 discontinuity. This is consistent with the topography we observe for this discontinuity.

The LVL above the 410 seems to be the result of hydration due to the presence of the subducted slab. In contrast to our observations in the Gulf of California, where a warm a hydrated system produced complex RsF, mainly for the 660 discontinuity, the RFs in central and southern Mexico seem simpler and suggest the presence of cold material.

Gulf of California (GoFC)

The 410- and the 660-discontinuities depth might be affected by velocity anomalies above or below them, but the TZ thickness is not (Lebedev et al., 2002). In most of the GoFC region this thickness is similar to the global average, except at the east of the gulf and around 29°N. The latter coincides with a low-velocity shallower anomaly previously observed in tomography studies and associated with the presence of fluids or melt (Zhang et al., 2007) and related to the slab windows that resulted from the cessation of Farallon.

North of 30°N, the upper mantle discontinuities seem complex; we discard multipathing since the observed topography is smooth and shows gradients of less than 30 km. On the other hand, a 140 K increase in temperature might enhance the garnet-perovskite transition seismic signature.

We mapped the upper mantle discontinuities by means of receiver functions. Three regions of the mantle transition zone can be distinguished along the Gulf of California axis based on their receiver functions and we can interpret them in terms of presence of water:

Discontinuity	Region - Thickness of Transition Zone		Ozonization (spreading through new ocean floor)
	Basin & Range Province	Rifting of continental crust	
410 km	Strong negative phase, suggest presence of LVL	Only positive phase, suggest presence of LVL	Negative phase and depressed positive phase.
520 km	Strong negative and positive phases.	Slightly thinner than global average.	Slightly thinner than global average. No evidence of 520. Slightly thinner than global average.
660 km	Multiple arrivals.	Double 660 phase.	Simple depressed 660 phase.
Interpretation	Complex region. Hydrated. Warm.	Dry system on the top and hydrated on the bottom. Warm.	Hydrated system on the top. Warm.

Figure 4. Topography of the 410 (top) and 660 (center) discontinuities. The color corresponds to the depth with respect to the mean depth. The bottom panel shows the transition zone thickness (TZT).

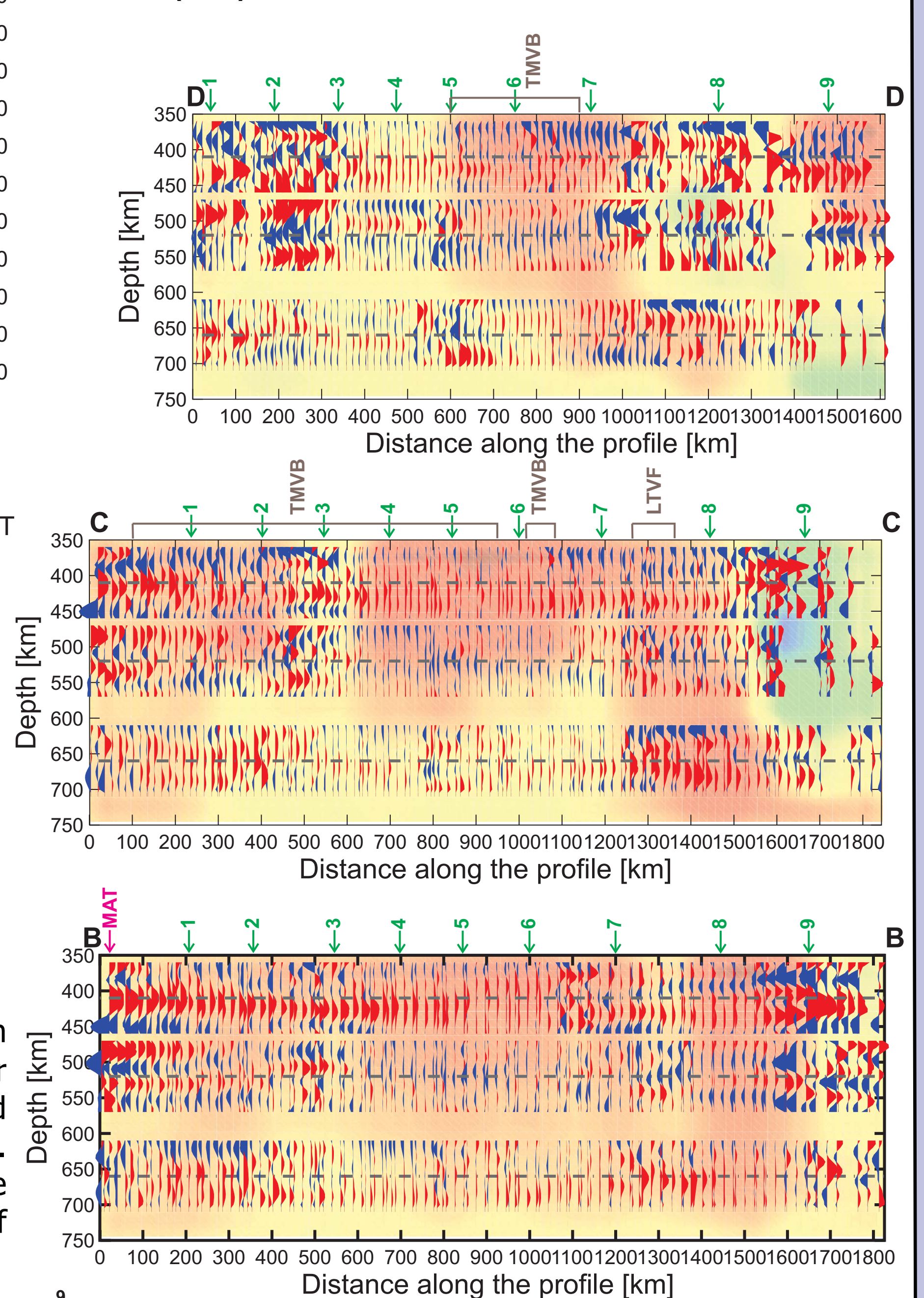


Figure 5. Profiles from west to east (1 to 9) and from south to north (a to d, see Fig. 1). The background color denotes the global tomography by Li et al. (2008), red for slower/warm regions and blue for fast/cold regions. The small numbers/letters on top of the profiles denote the position of the crossing profiles and the position of the TMVB along the profile.

REFERENCES

- Dueker, K. G. & Sheehan, A. F., 1997. Mantle discontinuity structure from midpoint stacks of converted P to S waves across the Yellowstone hotspot track, J. Geophys. Res., 102, 8313-8327.
- Efron, B. & Tibshirani, R. J., 1993. An introduction to the bootstrap, Monographs on statistics and applied probability, 57, Chapman & Hall/CRC, USA, pp.436.
- Gilbert, H. J., Sheehan, A. F., Dueker, K. G. & Molnar, P., 2003. Receiver functions in the western United States, with implications for upper mantle structure and dynamics, J. Geophys. Res., 108, B5-2299, doi:10.1029/2001JB001194.
- Gorbatov, A. & Fukao, Y., 2005. Tomographic search for missing link between the ancient Farallon subduction and the present Cocos subduction, Geophys. J. Int., 160, 849-854.
- Husker, A. & Davis, P. M. (2009), Tomography and thermal state of the Cocos plate subduction beneath Mexico City, J. Geophys. Res., 114, B04306, doi:10.1029/2008JB006039.
- Kennett, B. & Engdahl, E. R., 1991. Travel times for global earthquake location and phase identification, Geophys. J. Int., 105, 429-465.
- Kim, Y., Clayton, R. W. & Jackson, J. M., 2010. Geometry and seismic properties of the subducting Cocos plate in central Mexico, J. Geophys. Res., 115, B06310, doi:10.1029/2009JB006942.
- Li, C., van der Hilst, R. D., Engdahl, E. R. & Burdick, S., 2008. A new global model for P wave speed variations in Earth's mantle, Geochim. Geophys. Res., 9, Q05018, doi:10.1029/2007GC001806.
- Ligorria, J. P. & Ammon, C. J., 1999. Iterative deconvolution and receiver-function estimation, Bul. Seismol. Soc. Am., 89, 1395-1400.
- Melgar, D. & Pérez-Campos, X., 2011. Imaging the Moho and subducted oceanic crust at the Isthmus of Tehuantepec, Mexico, from receiver functions, Pure Appl. Geophys., DOI:10.1007/s00024-010-0199-5.
- Pardo, M. & Suárez, G., 1995. Shape of the subducted Rivera and Cocos plates in southern Mexico: Seismic and tectonic implications, J. Geophys. Res., 100, 12,357-12,373.
- Pérez-Campos, X., Kim, Y., Husker, A., Davis, P. M., Clayton, R. W., Iglesias, A., Pacheco, J. F., Singh, S. K., Manea, V. & Gurnis, M., 2008. Horizontal subduction and truncation of the Cocos Plate beneath central Mexico, Geophys. Res. Lett., 35, L18303, doi:10.1029/2008GL035127.
- Vinnik, L. P., 1977. Detection of waves converted from P to SV in the mantle, Phys. Earth planet. Inter., 15, 39-45.
- Wessel, P. & Smith, W. H. F., 1991. Free software helps map and display data, Eos Trans. AGU, 72(441), 445-446.

Acknowledgements

Figures were done using Generic Mapping Tools (GMT; Wessel & Smith, 1991). We thank all the volunteers that made possible the operation of MASE, VEOX, MARS, and CONA, and the SSN for their data. CONA stations were funded by Conacyt project 351566-F. Fund for this work was provided by the Tectonics Observatory at Caltech and DGAPA project IN105910.